Benefits of Preview Wind Information for Region 2 Wind Turbine Control

Ahmet Arda Ozdemir*, Peter Seiler† and Gary J. Balas‡
Department of Aerospace Engineering & Mechanics,
University of Minnesota, Minneapolis, MN, 55455, USA

The torque control of wind turbines in below-rated wind speeds involves a trade-off between power capture and generator loads. This paper explores this fundamental trade-off in the presence of preview wind information. A continuous-time optimal control problem is formulated on a one-state nonlinear turbine model. The numerical solution of this problem gives the Pareto optimal relationship between the gearbox loads and power capture. The effect of preview time and turbulence intensity on this optimal performance is investigated. This optimal performance is compared to the $K\omega^2$ standard control law. The main result quantifies the fact that the standard control law is not Pareto optimal. In other words, it is possible to use wind preview measurements to simultaneously increase power capture and decrease gearbox loads relative to the standard law. Moreover, the gap between the Pareto optimal performance and the standard law increases with the turbulence level.

Nomenclature

β	Blade pitch angle (deg)
λ	Tip-speed ratio (unitless)
ω_r	Rotor speed (rad/s)
ρ	Air density (kg/m^3)
τ_g	Generator Torque (Nm)
τ_{aero}	Aerodynamic Torque (Nm)
C_p	Power coefficient (unitless)
J	Inertia of the rotor and generator (kgm^2)
R	Turbine rotor radius (m)
v	Wind speed at hub-height (m/s)

I. Introduction

The $K\omega^2$ standard control law[1] is the most common method to control the turbine generator torque in below-rated (Region 2) wind conditions. The popularity of this law is mainly due to its simple design and relatively good power capture performance. In addition, this control law only requires a measurement of the rotor speed. However, it is not without its shortcomings. First, the standard law only yields the optimal power capture under steady wind conditions. Second, there is a fundamental trade-off between the gearbox loads and power capture. It is not clear if the standard control law is Pareto optimal in terms of this trade-off. In other words, it is unknown if there exists a different controller that can improve the power capture and lower the gearbox loads simultaneously. Finally, the standard law does not utilize preview wind measurements that can be obtained from advanced sensors such as LIDARs. These preview wind measurements can be used to alleviate the effects of wind fluctuations to improve the power capture and reduce gearbox loads.

*Doctoral Candidate: **arda@aem.umn.edu**
†Assistant Professor: **seiler@aem.umn.edu**
‡Professor: **balas@aem.umn.edu**

The trade-off between gearbox loads and the power capture can be seen in various work in the literature. For instance reference[1] describes a method that relies on the measurement of rotor acceleration. Authors report approximately 1% improvement in power capture, but with elevated swings in the generator torque that can be harmful for the gearbox. On the other hand, reference[2] uses a smaller gain in the standard law. Results show higher energy capture with lower generator torque in turbulent wind conditions. This result suggests that the standard law is not Pareto optimal since the lower generator torque is also likely to correspond to a lower gearbox load. The optimality of various Region 2 controllers in the literature is not quantified. Therefore it is not clear how far these controllers from the optimal in terms of the trade-off between the power capture and the gearbox loads.

In this paper we formulate a two-objective nonlinear optimal control problem that yields the Pareto optimal trade-off between the power capture and the gearbox loads in presence of preview wind information. The effect of the preview time and turbulence intensity on this trade-off is studied. The optimization problem is formulated in continuous-time based on a one-state rigid-body model of the National Wind Technology Center's (NWTC) Control Advanced Research Turbine 3 (CART3).[3] This optimization problem is solved numerically. The main result of this paper quantifies the fact that the standard control law is not Pareto optimal in turbulent wind conditions. It is also seen that the use of preview wind information can improve the power capture and reduce the drivetrain loads simultaneously.

The remainder of the paper is structured as follows: Section II details the formulation of the turbine optimal control problem. Section III analyzes the effect of the preview time and turbulence intensity on the optimal performance. Conclusions are presented in Section IV.

II. Problem Formulation

The power captured by the turbine rotor is approximately given by:

$$P_r = \frac{1}{2}\rho\pi R^2 v^3 C_p(\lambda,\beta) \tag{1}$$

where the power coefficient C_p that represents how much of the power available in wind is captured. C_p is a function of the blade pitch angle β (deg) and tip speed ratio $\lambda = \frac{\omega_r R}{v}$ (unitless). The $C_p(\lambda,\beta)$ data for CART3 is obtained from its high-fidelity model on the FAST simulation package. For Region 2 operation it is assumed that the turbine is being operated at the constant pitch angle β^* that yields the maximum C_p at the optimum tip speed ratio λ^*. Hence the C_p is simply denoted as $C_p(\lambda)$. The relationship between the rotor power P_r and the aerodynamic torque τ_{aero} is $P_r = \tau_{aero}\omega_r$. A one-state rigid-body turbine model that captures rotor dynamics can be written as:

$$\dot{\omega}_r = \frac{1}{J}(\tau_{aero} - \tau_g) \tag{2}$$

where the quantities J, τ_{aero} and τ_g are expressed as their low-speed shaft equivalents, i.e. on the rotor side of the gearbox. Substituting for τ_{aero} in Eq. (2) with $\frac{P_r}{\omega_r}$ gives:

$$\dot{\omega}_r = \frac{\rho\pi R^2 v^3 C_p(\lambda)}{2J\omega_r} - \frac{\tau_g}{J} \tag{3}$$

These nonlinear dynamics are denoted as $\dot{\omega}_r = f(\omega_r(t), \tau_g(t), t)$ for the remainder of the paper.

Flexible turbine gearboxes are often modeled as a mass-damper-spring system that connects the rotor and generator inertia. The damage in the gearbox is measured by the torque transmitted from the low-speed shaft to the high-speed shaft through the spring and the damper. The one-state model in Eq. 3 does not capture the flexible gearbox dynamics. However the variations in the generator torque τ_g closely represent the oscillations in the transmitted torque. Variations in τ_g are used as a measure of the gearbox damage in place of the more realistic damage-equivalent loads calculations based on the rotor shaft torque. This simpler model will be used for the formulation of the optimal control input.

The fundamental trade-off between the gearbox loads and power capture can be motivated as follows. Define C_p^* as the maximum power coefficient achieved at $\lambda^* = \frac{\omega_r^* R}{v}$. Assume there exists a generator torque input τ_g^* that maintains the turbine operating at constant λ^* and C_p^*. Substituting $C_p(\lambda)$, ω_r, $\dot{\omega}_r$ in Eq. (3) with C_p^*, $\frac{\lambda^* v}{R}$ and $\frac{\lambda^* \dot{v}}{R}$ respectively yields an analytical expression for the τ_g^*:

$$\tau_g^* = \frac{\rho\pi R^3 C_p^*}{2\lambda^*} v^2 - \frac{J\lambda^*}{R}\dot{v} \tag{4}$$

The τ_g^* that yields the maximum power capture is proportional to the square of the wind speed v and its rate of change. The variations in v^2 and $\dot{v}$ can be substantial in turbulent wind conditions. Figure 1 shows a simulation of the one-state model of the CART3 with τ_g^* and the standard control law $K\omega_r^2$ for a 600 (s) wind trajectory. The wind trajectory used in this simulation is obtained from NWTC's TurbSim[5] application. This wind trajectory closely represents the wind conditions at the CART3's site. It contained an average wind speed of 6 (m/s) and a turbulence intensity of 35%. CART3 is a 600 (kW) turbine with $R = 20$ (m) rotor radius located at the NWTC site at Boulder, Colorado. The values of the λ^* and C_p^* for CART3 are approximately 6 and 0.46. The top plot in Figure 1 shows the power coefficient C_p as a function of time and the bottom plot shows the generator torque demand during a gust. Over this 600 (s) period the τ_g^* yields more than 11% percent improvement in power capture over the standard law. However, the maximum torque that the generator of the CART3 can sustain is 3524 (Nm). The peak-to-peak torque swings of $1e7$ (Nm) seen with the τ_g^* cannot be realized. These type of large oscillations in τ_g create a large strain on the drivetrain. Moreover, the generator torque has large negative values that correspond to a large amount of electrical power drawn from the grid. It is of interest to understand this trade-off between the power capture and the drivetrain loads.

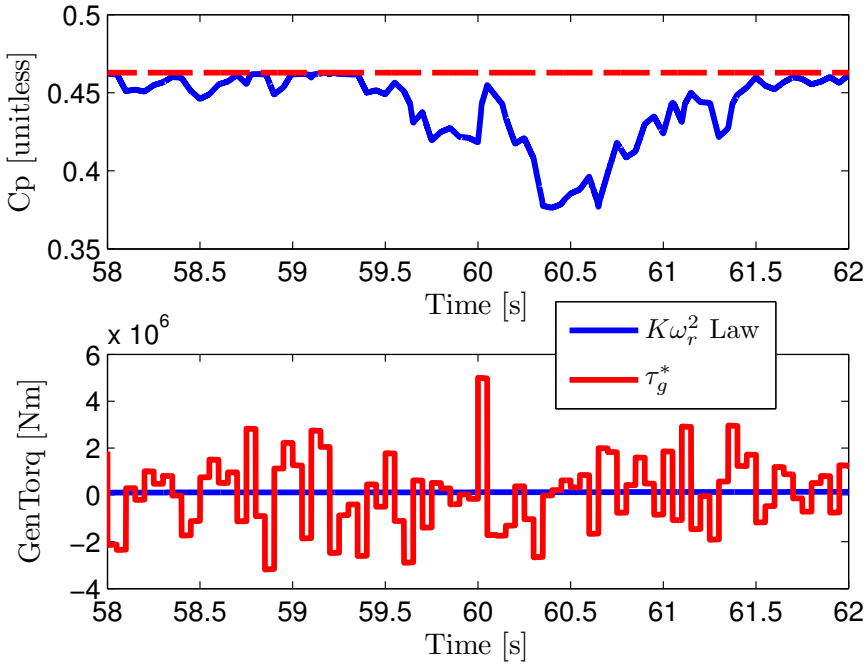

Figure 1. Control of the CART3 for the maximum power capture

The following optimal control problem is used to study the trade-off between the power capture and the drivetrain loads:

$$\begin{aligned} \underset{\tau_g(t)\in[0,T)}{\text{minimize}} \quad & \int_0^T \tau_g^2(t) - \alpha v^3(t) C_p(\lambda(t))\,\mathrm{d}t \\ \text{subject to:} \quad & \text{Equation (3)} \\ & \omega_r(0) = \lambda^* v(0)/R \end{aligned} \tag{5}$$

It is assumed that $v(t)$ in $t \in [0, T)$ is supplied by an advanced wind preview sensor such as a LIDAR. In words, the system is started at the rotor speed that yields the optimal power coefficient C_p^*. The turbulent wind conditions perturb the system from the optimal tip speed ratio that yield C_p^*. The $\tau_g(t)$ that minimizes the actuator use (τ_g^2) and maximizes the power capture ($v^3 C_p(\lambda)$) is being computed. Lower actuator use is correlated with lower gearbox loads. The coefficient α is the weight on the power capture. This weight can be changed to focus the optimization on the power capture or gearbox loads. Studying this optimization problem for a terminal time T corresponds to the use of T seconds of wind preview information for control.

Wind trajectories with different turbulence intensities can be used to analyze the effect of the turbulence on the optimal performance.

The optimization problem in Eq. 5 is a nonlinear optimal control problem with a fixed terminal time. Denote $L(\omega_r(t), \tau_g(t), t) = \tau_g^2(t) - \alpha v^3(t) C_p(\lambda(t))$. The solution of this problem should satisfy the following three optimality conditions:[6]

$$\begin{aligned} \dot{\omega}_r &= f(\omega_r(t), \tau_g(t), t) \\ \dot{\xi} &= -\left(\frac{\partial f}{\partial \omega_r}\right)^T \xi - \left(\frac{\partial L}{\partial \omega_r}\right)^T \\ 0 &= \left(\frac{\partial f}{\partial \tau_g}\right)^T \xi + \left(\frac{\partial L}{\partial \tau_g}\right)^T \end{aligned} \tag{6}$$

with boundary conditions $\omega_r(0) = \lambda^* v(0)/R$ and $\xi(T) = 0$. Here $\xi(t)$ are the multiplier functions.[6] This is a two-point boundary-value problem. The partial derivatives in Eq. (6) correspond to the following expressions for the turbine control problem defined in Eq. (5):

$$\begin{aligned} \frac{\partial f}{\partial \omega_r} &= -\frac{\rho \pi R^2 v^3 C_p(\lambda)}{2J\omega_r^2} + \frac{\rho \pi R^2 v^3}{2J\omega_r} \frac{\partial C_p(\lambda)}{\partial \omega_r} \\ \frac{\partial L}{\partial \omega_r} &= -\alpha v^3 \frac{\partial C_p(\lambda)}{\partial \omega_r} \\ \frac{\partial f}{\partial \tau_g} &= \frac{1}{J} \\ \frac{\partial L}{\partial \tau_g} &= 2\tau_g \end{aligned} \tag{7}$$

We solve this problem numerically to obtain the optimal control input τ_g over the time horizon of $t \in [0, T)$. This solution is obtained as follows. The variables in Eq. (6) (ω_r,τ_g,ξ) are discretized in time with sample time of T_s. The derivative terms on the left-hand side of the Eq. (6) are approximated via forward-differences, i.e. $\dot{\omega}_r(0) \approx (\omega_r(T_s) - \omega_r(0))/T_s$. Define $f_t = f(\omega_r(t), \tau_g(t), t)$. The three differential equations in (6) are converted to the following large nonlinear matrix equations:

$$\frac{1}{T_s}\begin{bmatrix} 1 & 0 & \dots & \dots & 0 \\ -1 & 1 & 0 & \dots & \vdots \\ 0 & \ddots & \ddots & \ddots & \vdots \\ \vdots & \ddots & \ddots & \ddots & 0 \\ 0 & \dots & 0 & -1 & 1 \end{bmatrix} \begin{bmatrix} \omega_r(T_s) \\ \omega_r(2T_s) \\ \omega_r(3T_s) \\ \vdots \\ \omega_r(T) \end{bmatrix} - \begin{bmatrix} \omega_r(0)/T_s \\ 0 \\ \vdots \\ \vdots \\ 0 \end{bmatrix} = \begin{bmatrix} f_0 \\ f_{T_s} \\ \vdots \\ \vdots \\ f_{T-T_s} \end{bmatrix} \tag{8}$$

$$\frac{1}{T_s}\begin{bmatrix} -1 & 1 & 0 & \dots & 0 \\ 0 & -1 & 1 & \ddots & \vdots \\ \vdots & \ddots & \ddots & \ddots & 0 \\ \vdots & \ddots & \ddots & \ddots & 1 \\ 0 & \dots & 0 & 0 & -1 \end{bmatrix} \begin{bmatrix} \xi(0) \\ \xi(T_s) \\ \xi(2T_s) \\ \vdots \\ \xi(T-T_s) \end{bmatrix} + \begin{bmatrix} 0 \\ \vdots \\ \vdots \\ 0 \\ \xi(T)/T_s \end{bmatrix} = -\begin{bmatrix} \frac{\partial f}{\partial \omega_r}\big|_{t=0} \xi(0) \\ \frac{\partial f}{\partial \omega_r}\big|_{t=T_s} \xi(T_s) \\ \vdots \\ \vdots \\ \frac{\partial f}{\partial \omega_r}\big|_{t=T-T_s} \xi(T-T_s) \end{bmatrix} - \begin{bmatrix} \frac{\partial L}{\partial \omega_r}\big|_{t=0} \\ \frac{\partial L}{\partial \omega_r}\big|_{t=T_s} \\ \vdots \\ \vdots \\ \frac{\partial L}{\partial \omega_r}\big|_{t=T-T_s} \end{bmatrix} \tag{9}$$

$$\begin{bmatrix} \xi(0) \\ \xi(T_s) \\ \xi(2T_s) \\ \vdots \\ \xi(T) \end{bmatrix} = 2J \begin{bmatrix} \tau_g(0) \\ \tau_g(T_s) \\ \tau_g(2T_s) \\ \vdots \\ \tau_g(T) \end{bmatrix} \tag{10}$$

The optimality conditions are simply nonlinear equations in ξ, ω_r and τ_g. A control problem with T seconds of preview discretized at sample time T_s corresponds to $3T/T_s + 1$ equations and unknowns. The

large matrix equations in Eqs. (8),(9) and (10) are numerically solved in MATLAB via trust-region methods. The $\xi(t)$ variables are eliminated from these equations before the solution by plugging Eq. (10) in Eq. (9). This eliminates $T/T_s + 1$ equations and unknowns. The analytical Jacobian of the resulting expressions are supplied to the numerical solver in MATLAB. The initial guess for the optimal ω_r and τ_g is obtained from simulation of the one-state model with the $K\omega_r^2$ law for the given wind trajectory. This optimization is solved in model predictive control style. In other words, these sets of equations are repeatedly solved at each simulation time step with the new wind data supplied from the preview wind sensor. At a preview time of $T = 15$ (s) and a sampling time of $T_s = 0.02$ (s) this problem contains $2T/T_s = 1500$ variables. Solution of one such optimization step takes less than 0.1 (s) on a typical desktop computer.

III. Optimal Performance Trade-Off

First we study the impact of the preview time on the optimal performance. A wind trajectory that represent the turbulence conditions at the CART3 site are generated with NWTC's TurbSim code. This trajectory is generated at an average wind speed of 6 (m/s) and has a turbulence intensity of 35%. $T = 15$, 30 and 600 (s) of preview times are investigated. Current preview wind sensors can typically supply wind information up to 200 (m) distance from turbines. This would approximately correspond to a 15 (s) of preview time with wind fluctuations around the average wind of 6 (m/s). The 30 (s) case investigates the benefits of extra preview. The 600 (s) preview case represents the limiting case where the full wind trajectory is available to the controller.

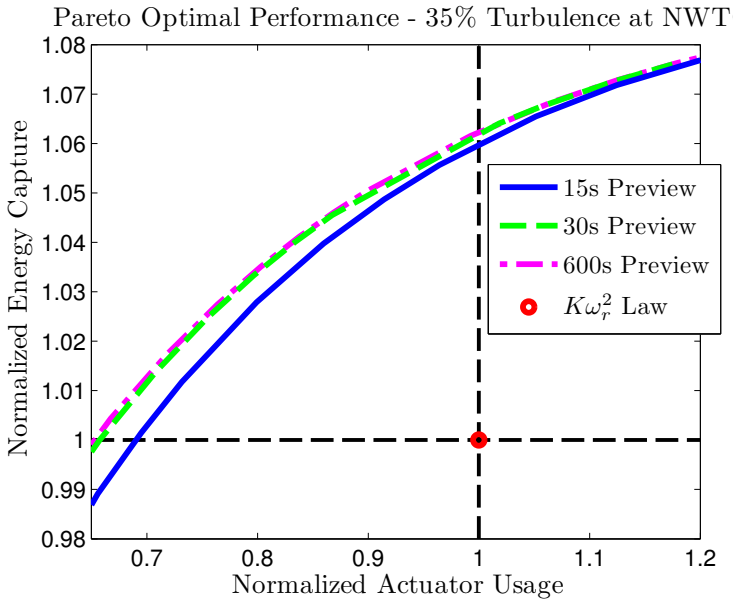

Figure 2. Pareto optimal performance trade-off with different preview times

The optimal problem in Eq. (5) is solved in model predictive control style over a simulation window of 600 (s). These simulations are run with different weights on energy capture (α in Eq. (5)) to capture the optimal trade-off between the power capture and the gearbox load reduction objectives. These performance metrics are normalized with respect to their respective values obtained with the $K\omega_r^2$ law for the same wind trajectory. Figure 2 presents the optimal performance trade-off with different preview times. It is seen that the 15 (s) preview is mostly sufficient for the optimal control action. This large preview time can be related to the inertia of the turbine rotor. It is challenging to make this inertia to respond to large wind gusts. Therefore it should be noted that larger turbines than the CART3 may require longer preview times. In the case of CART3, $T = 30$ (s) preview yield a limited performance improvement over the 15 (s) preview. This performance is almost optimal and the performance difference with the limiting 600 (s) preview case is negligible. It is also seen that a large performance improvement over the standard law can be obtained with the use of preview. A notable 6% improvement in power capture can be obtained while retaining similar

gearbox loads. Similarly a 30% load reduction can be obtained while achieving a similar power capture to the $K\omega_r^2$ law.

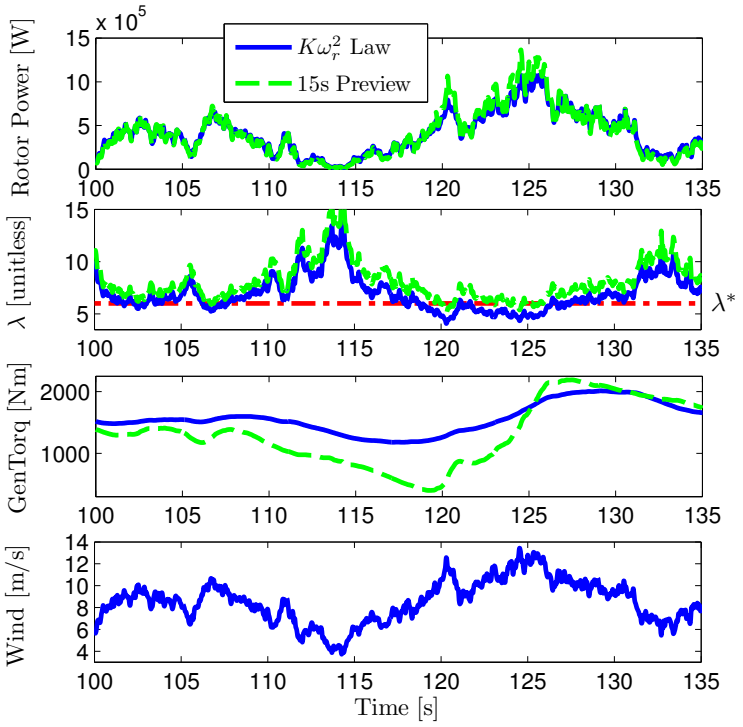

Figure 3. Time-domain plots of the standard control law and the model predictive controller

It is possible to gain some simple insight into controller behavior by analyzing time-domain results. The standard control law and the 15 (s) preview controller that yields the same gearbox loads are compared in Figure 3. This figure compares the power captured by the rotor, the tip speed ratio, the generator torque for the wind trajectory that is presented in the bottom plot. The optimal tip-speed ratio λ^* for CART3 is denoted with the red-dashed line in the tip-speed ratio plot. The wind trajectory contains a sharp drop in wind speed between $t \approx 105 - 115$ (s) and a gust that peaks at $t \approx 125$ (s). It is seen that the largest difference in the power capture is observed during the wind speed peaks. Both controllers spend similar amount of time close to the λ^*. However, the preview controller reaches this optimal tip speed ratio right at the moment of wind gust. The standard law attains the λ^* after the onset of the gust. The preview controller lowers the generator torque before the gust and increases the rotor speed. This leads to $\lambda > \lambda^*$. The λ drops to the λ^* when the wind gust hits the turbine. The captured power is proportional to the cube of the wind speed and it is more important to achieve λ^* during the wind gust. This behavior allows achieving λ^* when it matters most without introducing large generator torque swings.

The second problem we investigate is the effect of the turbulence level on the optimal performance. Three wind trajectories that have an average wind speed of 6 (m/s) and turbulence intensities of 35%, 22%, and 14% are considered. The 35% turbulent wind case corresponds to the wind conditions at the CART3 site. A realistic preview time of $T = 15$ (s) is considered. The model predictive controller defined in Eq. (5) is simulated over 600 (s) simulation windows. The normalized performance metrics are calculated for each wind trajectory. These results are presented in Figure 4. There are three key observations in Figure 4. First, the distance between the Pareto optimal front and the $K\omega_r^2$ law increases with increasing turbulence intensity. Second, simultaneous large improvements in power capture and reductions in gearbox loads can be obtained with use of preview. Third, sustaining a larger drivetrain damage than the $K\omega_r^2$ law in low-turbulent wind conditions yields limited power capture improvements. However, there is an important trade-off between the extra power capture and the loads with larger wind fluctuations. Whether a control method that yields higher power with higher loads is desirable depends on the extra cost incurred by the extra drivetrain damage. Development of cost models for turbine structures that relate the sustained damage to an economic cost is an open area of research.

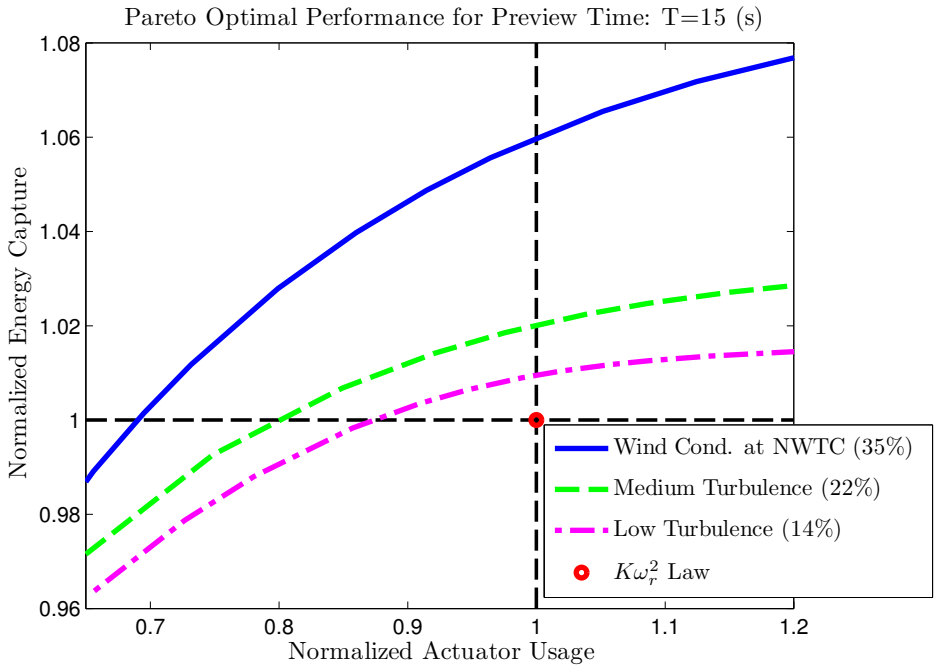

Figure 4. Pareto optimal performance trade-off with a fixed preview time of 15 (s)

IV. Conclusions

The analysis of the one-state turbine model quantifies the fact that the standard control law $K\omega_r^2$ is not Pareto optimal in turbulent wind conditions. In other words, there exists a control input for which power is increased and loads are reduced relative to the standard control law. Furthermore the distance between the Pareto optimal front and the $K\omega_r^2$ law increases with increasing turbulence intensities.

It is seen that the use of preview information in Region 2 control laws is a promising concept. In the ideal case an 6% extra power can be captured with similar gearbox loads seen with the standard law. Alternatively a 30% gearbox load reduction can be achieved over the $K\omega_r^2$ law with a similar power capture.

Acknowledgments

We would like to thank Alan Wright from National Renewable Energy Laboratory for supplying a model of the Controls Advanced Research Turbine (CART3).

This work was supported by the University of Minnesota Institute on the Environment, IREE Grant No. RL-0010-12 and the US Department of Energy Contract No. DE-EE0002980. Any opinions, findings, and conclusions or recommendations expressed in this material are those of the author(s) and do not necessarily reflect the views of the University of Minnesota or Department of Energy.

References

[1]Burton, T., Sharpe, D., Jenkins, N., and Bossanyi, E., *Wind Energy Handbook*, John Wiley & Sons, 1st ed., 2001.

[2]Johnson, K., Fingersh, L., Balas, M., and Pao, L., "Methods for increasing region 2 power capture on a variable-speed wind turbine," *Journal of solar energy engineering*, Vol. 126, 2004, pp. 1092.

[3]"CART3 FAST model, personal communication with A. Wright," 2011.

[4]Jonkman, J. M. and Buhl, J. M. L., *FAST User's Guide*, National Renewable Energy Laboratory, Golden, Colorado, 2005.

[5]Jonkman, B., *TurbSim User's Guide*, National Renewable Energy Laboratory, Golden, Colorado, 2009.

[6]Bryson, A. and Ho, Y., *Applied optimal control: optimization, estimation, and control*, Ginn and Company, 1969.

[7]Simley, E., Pao, L. Y., Frehlich, R., Jonkman, B., and Kelley, N., "Analysis of Wind Speed Measurements using Continuous Wave LIDAR for Wind Turbine Control," *49th AIAA Aerospace Sciences Meeting*, 2011, pp. AIAA–2011–263.

[8]Simley, E., Pao, L. Y., Kelley, N., Jonkman, B., and Frehlich, R., "LIDAR Wind Speed Measurements of Evolving Wind Fields," *50th AIAA Aerospace Sciences Meeting*, 2012, pp. AIAA–2012–656.